AUTOMATED BRAIN LESION CLASSIFICATION USING HYBRID FUZZY C-MEANS WITH CORRELATION TEMPLATE AND WAVELET TRANSFORM

Ayuni Fateeha Muda[a], Norhashimah Mohd Saad[a]*, Low Yin Fen[a], Abdul Rahim Abdullah[b], Nazreen Waeleh[a]

[a]Faculty of Electronics and Computer Engineering, Universiti Teknikal Malaysia Melaka, Hang Tuah Jaya, 76100 Durian Tunggal, Melaka, Malaysia
[b]Faculty of Electrical Engineering, Universiti Teknikal Malaysia Melaka, Hang Tuah Jaya, 76100 Durian Tunggal, Melaka, Malaysia

*Corresponding author
norhashimah@utem.edu.my

Graphical abstract
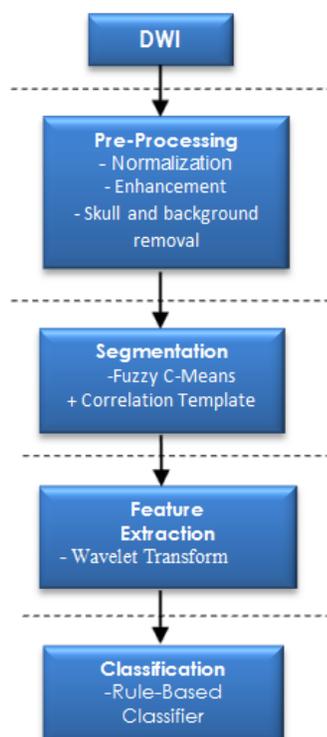
Abstract

This paper presents a new technique for automatically detecting and characterizing major brain lesions for diffusion-weighted imaging. The analytical framework consists of pre-processing, segmentation, features extraction and classification. For segmentation process, Fuzzy C-Means integrated with correlation template are proposed to detect the lesion region. The algorithm performance is evaluated using Jaccard and both false positive and false negative rates. Next, the features from wavelet transform are extracted from the region and fed into the rule-based classifier. Results demonstrated that FCM with correlation template offered the best performance for acute stroke segmentation with the highest rate of 0.77 Jaccard index. The classification accuracy for acute stroke, tumor, chronic stroke and necrosis are 94%, 97, 63% and 60%. In conclusion, the proposed hybrid analysis has the potential to be explored as a computer-aided tool to detect and diagnose of human brain lesion.

Keywords: Segmentation, brain lesion, Fuzzy C-Means (FCM), correlation template, wavelet

Abstrak

Kertas kerja ini mengusulkan teknik terbaru untuk mengesan dan mengkelaskan lesi otak utama untuk pengimejan magnetic resonan pemberat-serapan. Analisis rangka kerja bagi lesi otak terdiri daripada pra-pemproses, pengsegmenan, pengekstrakan ciri dan pengkelasan. Untuk proses pengsegmenan, Fuzzy C-Means bersepadu dengan template kolerasi dicadangkan untuk mengsegmen rantau lesi. Prestasi algoritma dinilai dengan menggunakan Jaccard and kedua-dua kadar palsu positif dan negatif. Kemudian, ciri ciri dari ubahan wavelet diekstrak daripada rantau dan diinputkan kepada pengelas berasaskan peraturan yang telah direka. Keputusan menunjukkan bahawa FCM dengan template korelasi mempunyai prestasi yang terbaik untuk segmentasi strok akut dengan 0.77 Jaccard index. Pengelasan ketepatan untuk strok akut, tumor, strok kronik dan nekrosis adalah 94%, 97%, 63% dan 60%. Sebagai kesimpulannya, analisis hybrid yang dicadangkan mempunyai potensi untuk diterokai sebagai alat bantuan komputer untuk mengesan dan mendiagnosis lesi otak manusia.

Kata kunci: Segmentasi, lesi otak, Fuzz C-Means (FCM), templat kolerasi, wavelet

1.0 INTRODUCTION

Recent years, the application of image processing methods has rapidly increased. Capturing and storing medical images are done digitally nowadays [1, 2]. Image segmentation is to divide the image into different regions according to given criteria for future process [2]. The key task in many medical applications is image segmentation [3]. There are lots of techniques for automatic and semi- automatic image segmentation but most of them fail in unknown noise, poor image contrast and weak boundaries which are usual in medical images. Medical images contain complicated structures and their accurate segmentation is necessary for clinical diagnosis [4].

The major trouble with medical segmentation is the accurate segmentation in improving the treatment and diagnosis of disease due to use of medical imaging techniques. Image segmentation becomes challenging and complex task because of the usual medical image has unknown noise and inhomogeneity [5]. The brain image segmentation is a complicated and challenging task that its precise segmentation is extremely important for detecting tumors, chronic stroke and necrosis [6]. Accurate detecting of these tissues is very significant in diagnostic systems. Magnetic resonance imaging (MRI) is an important imaging method for the detecting abnormal changes in different part of the brain in early stage [1].

Diffusion-weighted magnetic resonance imaging (DWI) has been widely applied in the medical image processing such as for a stroke, tumor and abscess [7]. The function of DWI is to measure the strength of water diffusion within a tissue structure like white matter (WM) and gray matter (GM), cerebral spinal fluid (CSF) and brain lesions (tumour, stroke n necrosis) that have their own particular diffusion character. Image contrast is based on the diffusivity character, where hyperintense is a lesion or tissues with low diffusion appear bright and hypointense is a lesion or tissues with high diffusion appear dark. Compared with MRI, DWI provides higher lesion contrast that considered as the most sensitive brain imaging detecting acute stroke. It useful in providing details of the lesions components [7]. In 2014, the estimated numbers of new brain cancers are increasing from 17,000 in 2009 to 23,380 in United States [8]. Ministry of Health Malaysia is reported in July 2012 the brain neoplasm (tumors) and cerebrovascular disease (strokes) are the third-and fourth-leading cause of death respectively in Malaysia [8].

Image segmentation techniques can be carved up into three categories such as boundary-based techniques, region-based techniques and pixel-based techniques; both are supervised and unsupervised. Fully automatic segmentation and the areas partition in feature space with high density is called unsupervised. The example of unsupervised is a feature-space based techniques, clustering and adaptive thresholding [9]. Region growing segmentation is based on intensity information or edges in the image [7]. An operator chooses a seed point manually and extracts all the pixels connected to the initial seed according to some specific criteria. The disadvantage of region growing is it sensitive to noise that can cause extracted regions to have holes or to be disconnected. The split and merge also called quad-tree segmentation that based on a quad-tree partition of an image. It is not a pixel based on segmentation [10].

Clustering is applied in the segmentation of images that can be used to unionize set of pixels into groups according to similarities among the individual data items in such a way that data points of the same group are more identical to one another than samples belonging to different groups. The fuzzy clustering technique is interesting to applied compare to hard clustering because it holds large information from the image. FCM provides flexibility that admits pixels to belong to multiple classes with changing degree of membership [11]. The disadvantage of FCM is unable to segment the image precisely because of the noise and inhomogeneity that it only considers clustering based on intensity only [12]. Three commonly applied clustering algorithms are k-means clustering, fuzzy c-means (FCM) and expectation maximization (EM) algorithms. EM performs the segmentation technique as a normal Gaussian distribution, but a noisy image is not a normal distribution generally [10,13,14]. To overcome the problem, a modified FCM is applied by incorporating the spatial neighborhood information into the standard FCM algorithm and modifying the membership weighting of each cluster [15].

Kwon and Han proposed a hierarchical FCM algorithm according to the template matching [16, 17] requirement for an accurate template. The segmentation efficiency of the FCM method is improved based on the cluster center initialization instead of random initialization by silhouette [16]. A parallel processing concept also implemented in FCM algorithm. It promises high speed processing but the hardware implementation is not effective. The clustering algorithm is implemented through quantization and aggregation by Esrich and KE that includes a weight factor for cluster center updating. The fast clustering algorithm based on random sampling that yields a speed-up factor proposed by Cheng and Godgof in 1998. Fuzzy C-Means (FCM) is a popular technique proposed by many researchers for segmentation of medical images [10]. However, noises and intensity inhomogeneity, FCM technique fail in producing accurate results. Although the original FCM algorithm provides good results for segmenting noise free images, it fails to segment images that are corrupted by noise, outlines and other imaging artifacts [11]. The FCM algorithm is modified to improve the part of the meaningful regions [9, 12]. Our theory is that it is feasible to automatically segment the hypointensity lesions in DWI by using Fuzzy C-means with template matching and dynamic contour. A brain classification system can be developed according to the features in DWI images.

This paper discusses automatic segmentation of brain lesions from DWI using Fuzzy C-means method

with correlation template and active contour. This paper has outlined as follows. The proposed methods are discussed in details in section II. Firstly, the section starts with flowchart of the proposed method. Then, the DWI used for this paper and description of the segmentation process. In section III, experimental results of applying the algorithm are used. In section IV, the conclusion is discussed.

2.0 MATERIALS AND METHODS

Figure 1 depicts the flowchart for the whole analysis. The samples of the brain DWI dataset are gathered first. Various algorithms are utilized for the pre-processing stage for normalization, background removal and intensity enhancement. Image segmentation algorithm is used in order to extract the region interest (ROI) of the lesion. Then, statistical measured is applied to measure the characteristics of the lesions. Lastly, rule-based classifier is performed to separate the type of brain lesion. The performance of the proposed techniques is evaluated according to the accuracy of the system.
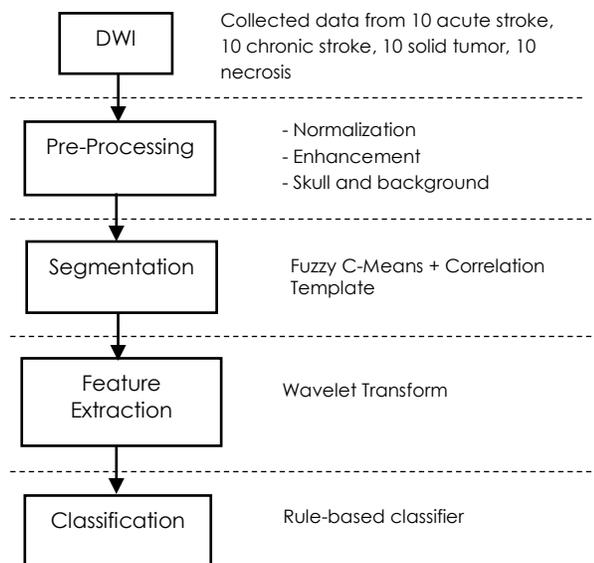
Figure 1 Flowchart of the Proposed System Design

2.1 Diffussion-weighted MRI

2.2.1 Image Dataset

The DWI images are collected from General Hospital of Kuala Lumpur using 1.5T MRI scanners Siemens Magnetom Avanto. The parameters obtained from this scanner are time echo (TE), 94ms; time repetition (TR), 3200ms; pixel resolutions, 256x256; slice thickness, 5mm; gap between each slice, 6.5 mm; intensity of diffusion weighting known as b value, $1000s/mm^2$ and total number of slices, 19. The data is encoded in 12-bit DICOM (Digital Imaging and Communication in

Medicine) format. The evaluation of the performance is based on the Area Overlap (AO), False negative rate (FNR) and False Positive Rate (FPR). The data set consists of 30 acute infarctions, 15 tumors, which are hyperintense lesions; 20 chronic strokes; 10 necrosis are hypointense cases. Overall, 75 images are used in the analysis. A portion of the data is used as training samples and the remaining data is for testing.

2.2.2 Brain Lesions

Brain lesions were segmented and marked manually by the specialist to perform the lesion area. Figure 2 portrays sample of the image obtained from this analysis. The lesion is indicated by a red circle. The region of normal brain consists of brain tissue also called as gray and white matter tissue in conventional MRI and the cavity which is full of cerebral spinal fluid (CSF) situated in the middle of the brain. The DWI intensity for CSF is dark. Several brain lesions are shown in Figure 2 (b-e) in which the intensity can be clustered into hyperintense and hypointense. The hyperintense lesions include acute stroke and tumor and hypointense lesions consists of chronic stroke and necrosis.

a) Normal   b)Acute stroke   c)Tumor

d) Stroke   e)Necrosis
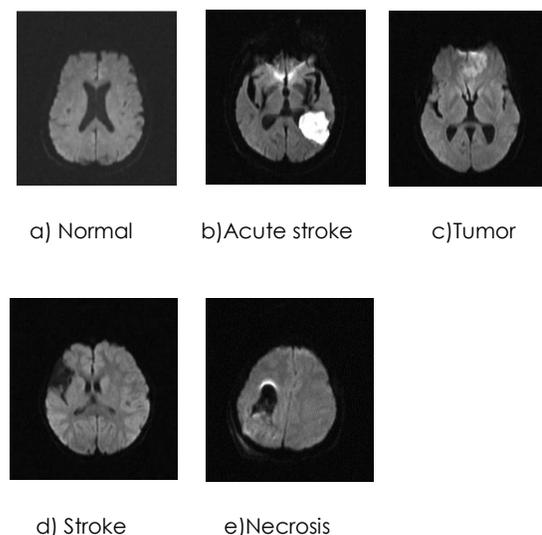
Figure 2 Image of DWI Lesions

2.2.3 Pre Processing Stage

Image preproc essing is the first stage in an image processing task. Various algorithms are applied for the pre-processing algorithms stage as in [8].

2.2.4 Segmentation
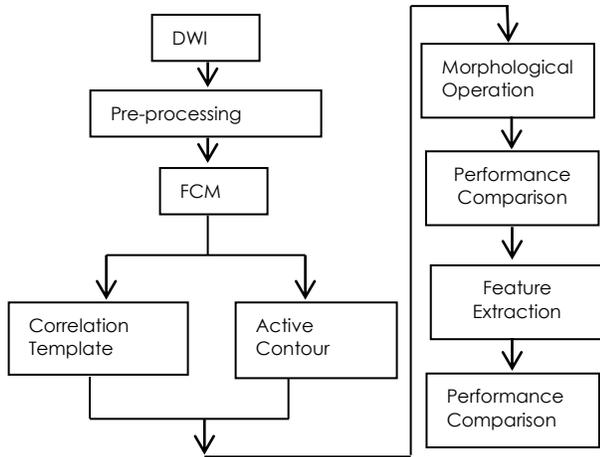
The flowchart of the proposed method is shown in Figure 3.

Figure 3 Flow Chart For FCM Proposed Method

Bezdek (1984) was the first researcher that proposed FCM algorithm. This algorithm widely used in the image segmentation [12,18]. This algorithm functions by assigning membership to each data point corresponding to each cluster center on the basis of distance between the cluster and the data point.

More the data is near to the cluster center more is its membership towards the particular cluster center. Summation of the membership of each data point should equal to one. The algorithm is based on minimization of the following objective function.

$$J_m = \sum_{i=1}^{N} \sum_{j=1}^{C} u_{ij}^m \|x_i - c_j\|^2 \ , 1 \leq m \leq \infty \tag{1}$$

where m (the fuzziness exponent) is any number greater than 1, N is a number of data, C is the number of clusters, u_{ij} is the degree of the membership of x_i in the cluster j, x_i is the ith of d-dimensional measured data, c_j is the d-dimension center of the cluster, and $\|*\|$ is any norm expressing the similarity between any measured data and center.

Fuzzy partition works through an iterative optimization of the objective function shown above, with the membership u_{ij} and the cluster centers c_j by:

$$u_{ij} = \frac{1}{\sum_{k=1}^{c} \left(\frac{\|x_i - c_j\|}{\|x_i - c_k\|} \right)^{\frac{2}{m-1}}} \tag{2}$$

where $\|x_i - c_j\|$ is the distance from point i to current cluster center j, $\|x_i - c_k\|$ is the distance from point i to the cluster center k.

$$c_j = \frac{\sum_{i=1}^{N} u_{ij}^m \cdot x_i}{\sum_{j=1}^{N} u_{ij}^m} \tag{3}$$

The iteration will stop when

$$max_{ij} \left\{ | u_{ij}^{k+1} - u_{ij}^{(k)} | \right\} < \varepsilon \tag{4}$$

where ε is a termination criterion between 0 and 1, whereas k is the iteration step. This procedure converges to a local minimum or a saddle point J_m.

At each iteration, the algorithm can be finished in two steps which are the first step includes computing the fuzzy membership function. Second, the algorithm calculates the values of cluster centers. The cluster centers are initialized to random values ranged between maximum and minimum intensity level since the unknown variables regarding the cluster centers and fuzzy membership arrays cannot be computed directly. To estimate cluster centers and fuzzy membership values in the desired accuracy, the algorithm exploits its iterative. When the difference between two clusters at two successive iterations is less than a small value of ε, the stopping criterion for an algorithm is met. The algorithm is composed of the following steps:

1. Select cluster center
2. Initialize the membership matrix U with random values between 0 and 1.

$$U = [u_{ij}] \text{ matrix, } u^{(0)} \tag{5}$$

Calculate the u_{ij} by using this equation:

$$u_{ij} = \frac{1}{\sum_{k=1}^{c} \left(\frac{\|x_i - c_j\|}{\|x_i - c_k\|} \right)^{\frac{2}{m-1}}} \tag{6}$$

3. At k-step: calculate the centers vectors $C^{(k)} = [c_j]$ with $U^{(k)}$

$$c_j = \frac{\sum_{i=1}^{N} u_{ij}^m \cdot x_i}{\sum_{j=1}^{N} u_{ij}^m} \tag{7}$$

4. Update $U^{(k)}$, $U^{(k+1)}$

$$u_{ij} = \frac{1}{\sum_{k=1}^{c} \left(\frac{\|x_i - c_j\|}{\|x_i - c_k\|} \right)^{\frac{2}{m-1}}} \tag{8}$$

5. If $\|U^{(k+1)} - U^{(k)}\| < \varepsilon$ or the minimum J is achieved, then STOP. Otherwise, return to step 2.

The Morphological operation is used to get rid of the dissonance in the picture after segmentation process. To get rid of the commotion and the result become more precise, both algorithms need to employ this technique. Binary area open is applied to remove unwanted pixels less than 100 for hyperintense and 200 for hypointense. BW2 = bwareaopen (BW, P) removes from a binary image all connected parts (objects) that have pixels less than P pixels. It will produce some other binary image BW2. The value is set at 100 for hyperintense and 200 for hypointense.

Hypointense is one of the problems by using the FCM algorithm. One of the way to encounter this problem is by using correlation coefficient template [17]. The major problem with this algorithm is the value of the intensity between the lesion and the CSF is quite similar. Thus, the algorithm is unable to segment accurately and start out worse.

2.2.5   *Correlation Template*

In hypointense lesions, the intensity of the lesion and the CSF are in the middle of the brain DWI is similar. Therefore, FCM cannot differentiate between these clusters and unable to segment the hypointense lesion precisely. The performance of result can be improved by using correlation template (refer Figure 4)to remove the CSF area [17].
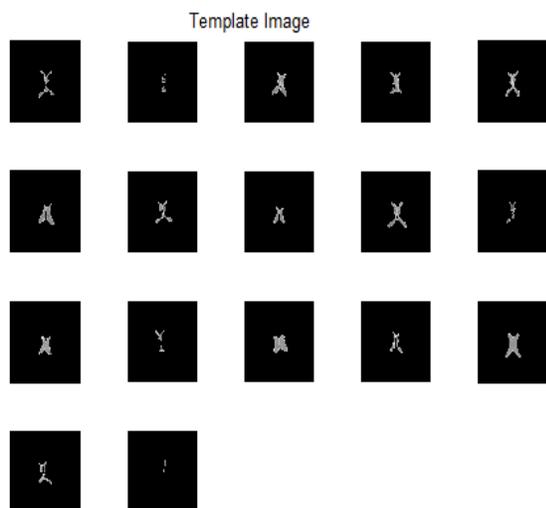

Figure 4 Template CSF for normal image

Correlation quantifies the extent to which two quantitative variables, X and Y, "go together". When high values of X are associated with high values of Y, positive correlation existed while higher values of X are associated with low values of Y, the negative correlation exists. The correlational strength cannot judge by the eye. The abnormal image need to compare with normal images first in order to see the CSF characteristic. Three different sums of square (SS) are required to estimate a correlation coefficient which is the sums of squares for variable X, the amount of square variable Y and the sum of square variable of XY.The total of squares for variable X is:

$$ss_{XX} = \sum (x_i - \bar{x})^2 \tag{9}$$

The statistic keeps track of the spread of variable X. This statistic is the numerator of the variance of X ($s^2{}_x$), it can be calculated as:

$$(s^2{}_x)\,(n\text{-}1) \tag{10}$$

The sum of squares for variable Y is:

$$ss_{YY} = \sum (y_i - \bar{y})^2 \text{ or } (s^2{}_Y)\,(n\text{-}1) \tag{11}$$

The sum of the cross-product (SS$_{XY}$) is:

$$ss_{XY} = \sum (x_i - \bar{x})\,(y_i - \bar{y}) \tag{12}$$

This statistic is analogous to the other sums of squares except that it is used to quantify the extent to which the two variables "go together". The correlation coefficient (r) is

$$r = \frac{SS_{XY}}{\sqrt{(SS_{XX})(SS_{YY})}} \tag{13}$$

The sign of the correlation identifies whether the correlation is positive or negative. The firm of the correlation is known based on the magnitude of the correlation coefficient. I [hesitatingly] offer the guidelines because there are no hard and fast rules for describing correctional strength. For $0 < |r| < 0.3$ is weak correlation, $0.3 < |r| < 0.7$ is moderate correlation and when $|r| > 0.7$ is strong correlation. There are numbers of normal image clinical sample gathered in the template. The template which is used to remove CSF image is selected when the value of r is high. After the template is selected, the process is continued to perform the segmentation result. The equation that is used to get the result is:

$$X = P_{i(x,y)} - P_{2(x,y)} \tag{14}$$

where $P_{i\,(x,y)}$ is sample of image and $P_{2\,(x,y)}$ is the template image.

2.2.6   *Features Extraction*

Feature extraction is applied to present the characteristics of lesion parameter such as mode, standard deviation, mean, median and mean of the boundary. The continuous wavelet transform (CWT) algorithm can be shown below:

1. The wavelet is taking and compared to section at the start of the original signal.
2. The number C is calculated to know the close between related wavelet and signal.
3. The wavelet is shifted to the right and the step and 2 is repeated for the whole signal.
4. The scale wavelet is stretched and the step 1 to 3 is represented.
5. Lastly, step 1 to 4 is repeated for all scale.

CWT detects smooth signal features and produce large wavelet coefficient at scales where the oscillation in the wavelet correlate best with signal feature.

After segmentation process, the image is crop based on the shape of the lesions. Then, the image is converted to 64x64 pixels from 256 x 256 pixels to fix the size. Every image is transformed to signal. Last but not least, it will convert to CWT. It possess the ability to construct a time-frequency representation of a signal that offers very good time and frequency localization. Continuous wavelet transform of a function x(t) at a scale (a>0) a∈R† translate value b∈R

$$X_w\,(a,b) = \frac{1}{|a|^2} \int_{-\infty}^{\infty} x(t)\Psi\left(\frac{t-b}{a}\right) dt \tag{15}$$

$\Psi(t)$ = continous function in both the time domain and frequency domain (mother wavelet).

At this stage, the significant difference is tested by using anova method. The function of anova is to find the difference between the abnormal and normal signal. If there is a value when the comparison between abnormal and normal signal is made, so, the hypothesis is accepted. After that, we continue the research find the features by using median, mean, variance and standard deviation. The equations that are applied to each pixel are following:

$$\text{Mean} = \cup = \frac{\sum X}{N} \tag{16}$$

$$\text{Variance} = S2 = \frac{\sum (X - \bar{X})^2}{n-1} \tag{17}$$

$$\text{Standard Deviation} = \sqrt[S]{S^2} \tag{18}$$

The features measured are shown in Figure 5 and Figure 6. These figures show two dimensional (2-D) plots of wavelet transform from the ROI. The plots show obvious distinction in clusters between acute stroke and tumor. Acute stroke and tumor are represented by blue and green while necrosis and chronic stroke are represented by red and cyan respectively.

During the classification stage, a rule-based classifier is applied [21,22]. This is based on its simplicity as well as its ability to do multi-classification of many input features. The combinations of these features can differentiate the described lesions. The overall process of lesion classification is portrayed in the flowchart in Figure 7.
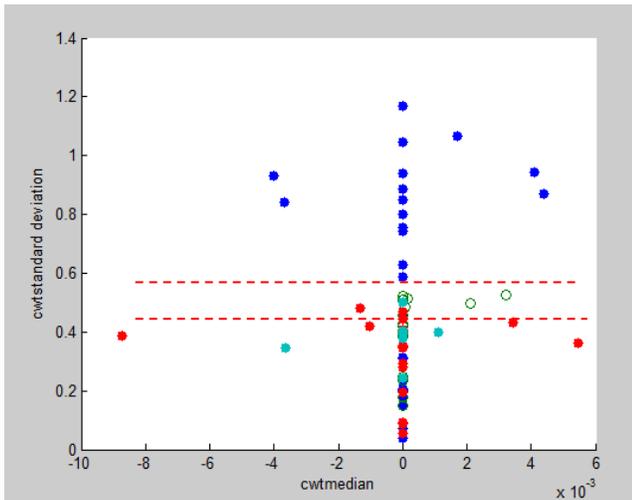

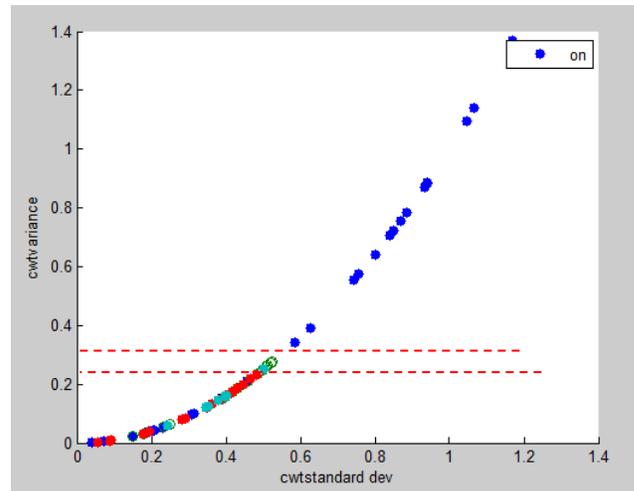**Figure 5** Distributions of Standard deviation and Median in Wavelet

Figure 6 Distributions of Variance and Standard Deviation in Wavelet

2.2.7   *Performance Evaluation*

The segmentation results obtained from the proposed technique are compared with the manual reference segmentation images, drawn by neuro-radiologists. Area overlap (AO) based on Jaccard's index is applied to measure the accuracy of the segmentation for the pair of segmented and reference image [7]. The range is from 0 which is no overlap and 1 for complete congruence. The advantage of Jaccard's overlap ratio is insensitive to over-under-segmentation estimations. Therefore, to evaluate the error measure, false positive rate (FPR, over segmentation error) and false negative rate (FNR, under segmentation error) are also calculated using the following metrics [7]:

$$AO = \frac{A \cap G}{A \cup G} \tag{19}$$

$$FPR = \frac{A \cap G^c}{A \cup G} \tag{20}$$

$$FNR = \frac{A^c \cap G}{A \cup G} \tag{21}$$

where A represents the segmentation results obtained by the proposed algorithm and G represents manual reference segmentation. *AO* computes Jaccard's overlap ratio between the segmentation and the manual reference. FPR and FNR are applied to quantify over- and under-segmentation respectively. High AO and low FPR and FNR show high accuracy and low error of the measurement. Accuracy of the correct classification is evaluated using equation (23).

$$Accuracy = \frac{\sum correct\ classification}{\sum number\ of\ sample} x\ 100 \tag{22}$$
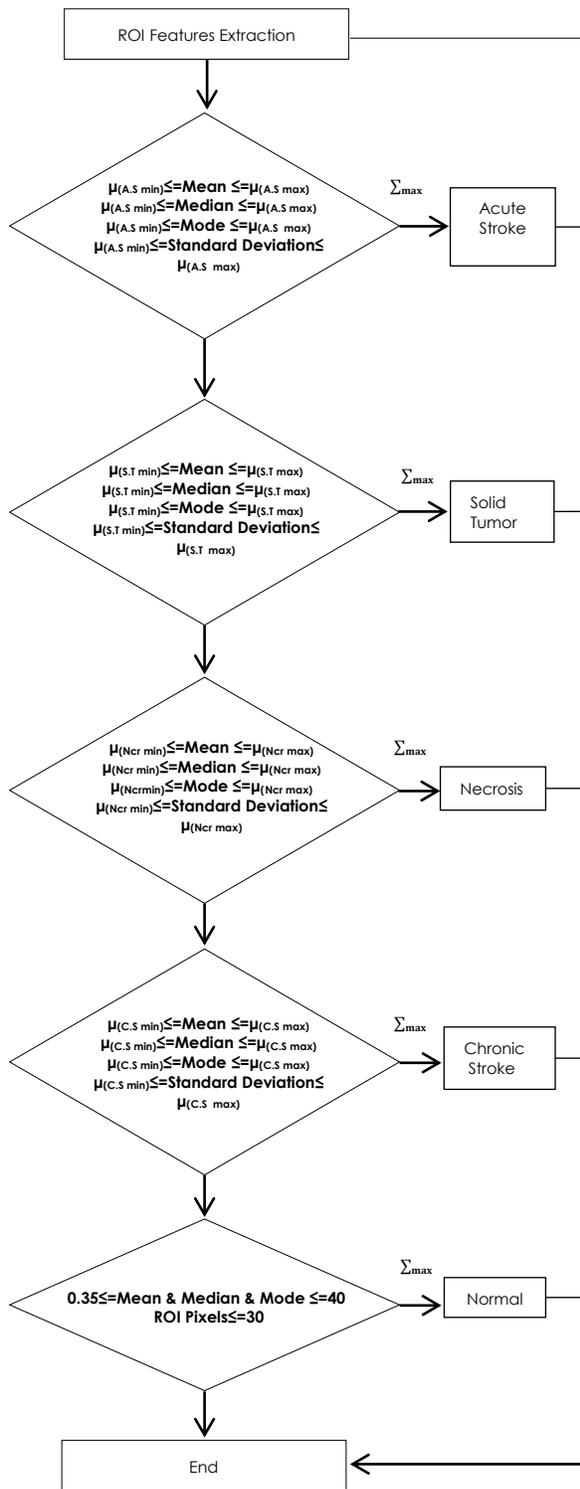
Figure 7 Rule-based Classification Process

3.0 RESULTS AND DISCUSSION

3.1 Segmentation Performance and Error Rates

The suggested algorithm is examined in several DWI with some cases of lesions like acute stroke, tumors,

chronic stroke and necrosis. The hyperintense and hypointense lesions and their segmentation are presented in Figure 11. The lesion's area is indicated by the red circle in the original image in Figure 8.

Figure 9 portrays the hyperintensity lesions for acute stroke and tumors. The results show that FCM can successfully segment the hyperintensity lesions while for hypointense which is for chronic stroke and necrosis, FCM need to combine with correlation template or active contour. It is because the FCM method fails to locate the area of the lesions. The cerebral spinal fluid (CSF) is situated in the middle of the brain, that it shares a similar intensity range with lesions and is segmented as the lesion's region. So, from the above result, by using correlation template, the FCM provides more accurate segmentation compare to active contour [23]. The result can be shown in Figure 10.
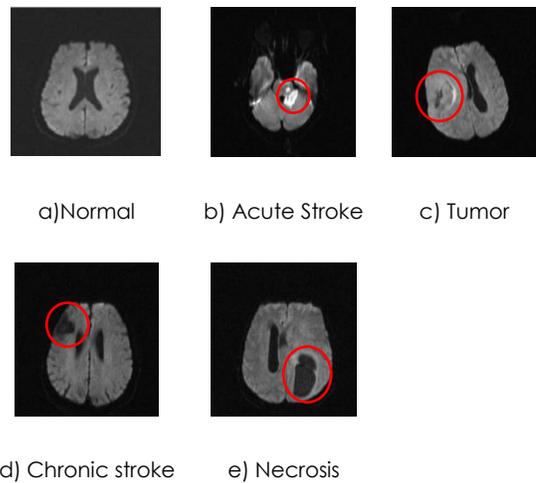

a)Normal   b) Acute Stroke   c) Tumor

d) Chronic stroke   e) Necrosis

Figure 8 Original DWI with brain lesion indicated by a red circle

DWI   FCM Result   Manual Reference

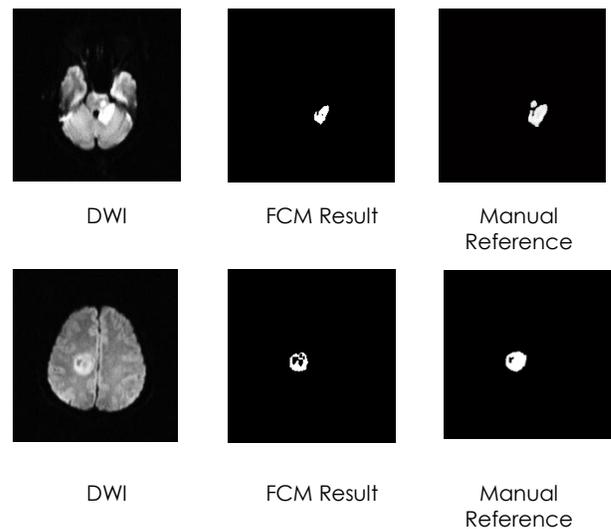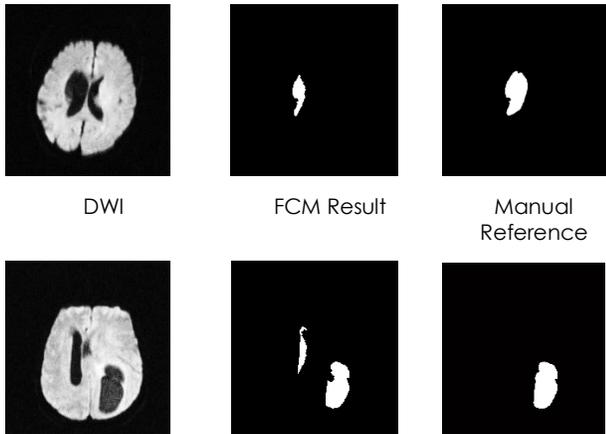DWI   FCM Result   Manual Reference

Figure 9 Hyperintensity Lesions using FCM and Manual Reference

Figure 10 Hypointensity Lesions using FCM with Correlation Template and Manual Reference

The performance of the FCM segmentation method is shown in Table 1 and Table 2. The results depend on 10 sample images for each type of lesions. To perform manual reference, each manual segmentation image needs to be handled by experts. The results show that for a hyper-intensity lesion, the overlap ratio rate is above 0.5, which is 0.78 for acute stroke, and for solid tumor is 0.64. The FPR and FNR error are low which are for acute stroke 0 and 0.23; and for tumor 0.07 and 0.28 for solid tumor, respectively. From the results, solid tumor depicts lower segmentation results compared to acute stroke. This is because the lesion region is irregular and partially blurry compared than acute stroke; the lesion is high intensity and has clear boundaries.

For hypointensity, the correlation template and active contour are applied to get accurate results. This is due to the inability of the method to characterize the intensity between lesions and CSF. CSF shares similar hypointensity and situated in the middle of the brain. It is symmetric and the area is big, so resulting in over segmentation error. The Jaccard's overlap ratio for a correlation template for chronic stroke is 0.51, while necrosis is 0.47. FPR and FNR for chronic stroke are 0.37 and 0.11 and for necrosis is 0.33 and 0.19. The average segmentation performance of correlation template are 0.598 (Jaccard's overlap ration); 0.195 (false positive rate); and 0.204 for false negative rate. For active contour, the Jaccard's overlap ratio for chronic stroke is 0.50, while necrosis is 0.37. For FNR, chronic stroke is 0.22 and 0.1 for necrosis. FPR are 0.28 (chronic stroke) and 0.31 (necrosis). FCM with template correlation provides better performance for chronic stroke and necrosis compare to active contour [23]. Jaccard's similarity index of the segmentation results for correlation template for acute stroke, solid tumor, chronic stroke and necrosis are 0.77, 0.65, 0.51 and 0.47 compare to active contour is 0.77, 0..65, 0.50 and 0.37, respectively.

3.2 Classification Performance and Accuracy

The confusion matrix for the classification results is shown in Table 3. This experiment is performed by training classifier by 90% of samples, using a simple static split data. The rest of the samples (75 images) are applied for testing the classifier. The best classification performance is obtained for acute stroke which is composed of hyperintensity features. Furthermore, for hypointensity classification, the correlation template gives high performance results compare to active contour. Correct classification is achieved at 0.94, 0.97, 0.78 and 0.7 for acute stroke, tumor, chronic stroke and necrosis.

The classification rate for the automatic system is shown in Figure 11. The results of correct classification are 94% and 97% for acute stroke and tumor; 63% and 60% for chronic stroke and necrosis. It is shown that the automated classification accuracy is comparable to the manual reference. Overall, FCM segmentation provides accurate segmentation performance for both hyper- and hypo- intensity lesions. By utilizing a rule-based classification approach, four types of lesions in DWI can be characterized.

Table 1 Segmentation evaluation of correlation template

Lesions	Performance Index		
	Jaccard's Overlap Ratio (Area Overlap)	False Positive (FPR-Over Segmentation Error)	False Negative (FNR-Under Segmentation Error)
Acute Stoke	0.767	0	0.234
Tumor	0.647	0.075	0.278
Chronic Stroke	0.510	0.375	0.115
Necrosis	0.469	0.329	0.190
Average	0.598	0.195	0.204

Table 2 Segmentation evaluation of active contour [23]

Lesions	Performance Index		
	Jaccard's Overlap Ratio (Area Overlap)	False Positive (FPR-Over Segmentation Error)	False Negative (FNR-Under Segmentation Error)
Acute Stoke	0.767	0	0.234
Tumor	0.647	0.075	0.278
Chronic Stroke	0.495	0.281	0.224
Necrosis	0.370	0.309	0.099
Average	0.570	0.166	0.208

Table 3 Results of confusion matrix 90% state split data for correlation template

Predicted	Actual					
	Acute Stroke	Tumor	Chronic Stroke	Necrosis	Normal	Correct Classification
Acute Stoke	0.94	0.03			0.03	0.94
Tumor	0.03	0.97				0.97
Chronic Stroke	0.11		0.78	0.11		0.78
Necrosis			0.2	0.7	0.1	0.7
Normal						1

4.0 CONCLUSION

A new DWI analysis method for segmentation and classification of brain lesions is demonstrated in this research. FCM and rule-based classifier is the method of applying to develop an automated brain classification system. The performance of the segmentation method is evaluated and discussed. Jaccard's similarity index of the segmentation results is 0.77, 0.65, 0.51 and 0.47. For the classification accuracy is 94% and 97% for acute stroke and tumor; 63% and 60%. So, correlation template provides high performance classification for hyperintensity and hypointensity lesions.
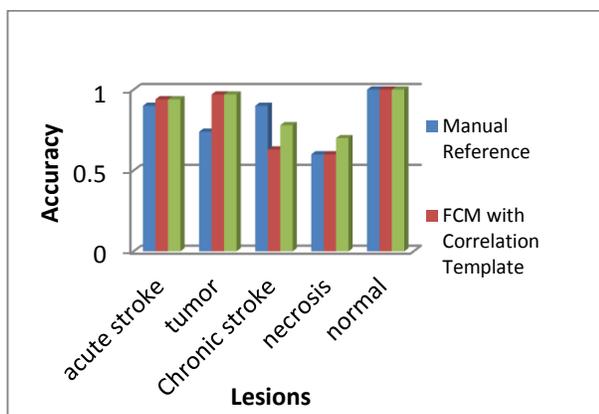
Figure 11 Classification Accuracy for Manual and FCM with Template Correlation and Active Contour

Acknowledgement

References

[1] Balafar, M. A., A. R. Ramli, M. I. Saripan, and S. Mashohor. 2008. Medical Image Segmentation using Fuzzy C-Mean (FCM), Bayesian Method and User Interaction. *IEEE International Conference on Wavelet Analysis and Pattern Recognition. ICWAPR'08.* 1: 68-73.

[2] Chang, P. L., and W. G. Teng. 2007. Exploiting the Self-Organizing Map for Medical Image Segmentation. *Twentieth IEEE International Symposium on Computer-Based Medical Systems. CBMS'07.* 281-288.

[3] Balafar, M. A., A. R. Ramli, M. I. Saripan, R. Mahmud, S. Mashohor, and M. Balafar. 2008. New Multi-Scale Medical Image Segmentation Based on Fuzzy C-Mean (FCM). *IEEE Conference on Innovative Technologies in Intelligent Systems and Industrial Applications.* 66-70.

[4] Hall, L. O., A. M. Bensaid, L. P. Clarke, R. P. Velthuizen, M. S. Silbiger, & J. C. Bezdek. 1992. A Comparison of Neural Network and Fuzzy Clustering Techniques in Segmenting Magnetic Resonance Images of the Brain. *Neural Networks, IEEE Transactions on,* 3(5): 672-682.

[5] Kannan, S. R., R. Pandiyarajan, And S. Ramathilagam. 2010. Effective Weighted Bias Fuzzy C-Means in Segmentation of Brain MRI. *International Conference on Intelligent and Advanced Systems (ICIAS), 2010.* 1-6.

[6] Bandhyopadhyay, D. S. K., and T. U. Paul. 2012. Segmentation of Brain MRI Image–A Review. *International Journal of Advanced Research in Computer Science and Software Engineering.* 2(3).

[7] Norhashimah, M. S., A. R. Abdullah. 2012. Fully Automated Region Growing Segmentation of Brain Lesion in Diffusion-Weighted MRI. *IAENG International Journal of Computer Science.* 39(2): 155-164.

[8] Norhashimah, M. S., A. R. Syed, A. F. Muda, M. Sobri. 2014. Automatic Brain Lesion Detection and Classification Based on Diffusion-Weighted Imaging using Adaptive Thresholding and a Rule-Based Classifier. *International Journal of Engineering and Technology.* 6(6): 2685-2697.

[9] Christ, M. J., and R. M. S. Parvathi. 2011. Segmentation of Medical Image using Clustering and Watershed Algorithms. *American Journal of Applied Sciences.* 8(12): 1349.

[10] Ayuni, F. M., M. S. Norhashimah, S. A. R. Abu Bakar. 2015. Brain Lesion Segmentation using Fuzzy C-Means on Diffusion-Weighted Imaging. *ARPN Journal of Engineering and Applied Sciences.* 10(3): 1138-1144.

[11] Badmera, M. S., A. P. Nilawar, and A. R. Karwankar. 2013. Modified FCM Approach for MR Brain Image Segmentation. *IEEE Conference on Circuits, Power and Computing Technologies (ICCPCT).* 891-896.

[12] Majd, E. M., M. A. As' Ari, U. U. Sheikh, and S. A. R. Abu-Bakar.. 2012. Hybrid Image Segmentation using Fuzzy C-Means and Gravitational Search Algorithm. *Fourth International Conference on Digital Image Processing (ICDIP 2012)* . International Society for Optics and Photonics. 83342V-83342V.

[13] Ahirwar, A.. 2013. Study of Techniques used for Medical Image Segmentation and Computation of Statistical Test for Region Classification of Brain MRI. *International Journal of Information Technology and Computer Science (IJITCS).* 5(5): 44.

[14] Dokur, Z. 2008. A Unified Framework for Image Compression and Segmentation by using an Incremental Neural Network. *Expert Systems with Applications.* 34(1): 611-619.

[15] Anandgaonkar, G. P., and G. S. Sable. 2013. Detection and Identification of Brain Tumor in Brain MRI using Fuzzy C-Means Segmentation. *International Journal of Research in Computer and Communication Engineering.* 2(10).

[16] Shasidhar, M., V. S. Raja, and B. V. Kumar. 2011. MRI Brain Image Segmentation using Modified Fuzzy C-Means Clustering Algorithm. *IEEE International Conference on Communication Systems and Network Technologies (CSNT).* 473-478.

[17] Kwon, M.,Y. Han, H. Park, and I. H. Shin. 2003. Segmentation of Brain MR Image using Template Matching and Hierarchical Fuzzy C-Means Algorithm. *International Society for Magnetic Resonance in Medicine (ISMRM) 13.*

[18] Bezdek, J. 1981. *Pattern Recognition with Fuzzy Objective Function Algorithms.* New York: Plenum Press.

[19] Li, C., R. Huang, Z. Ding, C. Gatenby, D. Metaxas, & J. Gore. 2008. A Variational Level Set Approach to Segmentation and Bias Correction of Images with Intensity Inhomogeneity. In *Medical Image Computing and Computer-Assisted Intervention–MICCAI.* Springer Berlin Heidelberg. 1083-1091.

[20] Li, C., C. Xu, C. Gui, and M. D. Fox. 2010. Distance Regularized Level Set Evolution and Its Application to Image Segmentation. *IEEE Transactions on Image Processing,* 19(12): 3243-3254.

[21] Zaıane, O. R., M. L. Antonie, and A. Coman. 2002. Mammography Classification by an Association Rule-Based Classifier. Proceeding *MDM/KDD: Int. Workshop Multimedia Data Mining.* 62-69.

[22] Duda, R., P. Hart and D. Stork. 2001. *Pattern Classification.* New York: Wiley.

[23] Muda, A. F., N. M. Saad, N. Waeleh, A. R. Abdullah and L. Y. Fen. 2015. Integration of Fuzzy C-Means with Correlation Template and Active Contour for Brain Lesion Segmentation in Diffusion-Weighted MRI. *IEEE 3rd International Conference on Artificial Intelligence, Modelling and Simulation, AIMS2015.*